CHAPTER 2

LITERATURE REVIEW

2.1 INTRODUCTION

In this chapter, the literature review on the proposed topic of texture analysis is presented pertaining to our research work.

Texture analysis is an important and useful area of study in machine vision. Its application ranges from ground cover identification in satellite images to detection of benign and malignant tissues in medical images. This chapter covers the major approaches of texture analysis, various studies and observations reported in literature and the applications of texture analysis methods. The main objective in texture analysis is to use a suitable unique descriptor to characterize and obtain features.

Texture is one of the vital information tools for identification and classification of objects. The basic requirement for a region to be considered as textured, is that there should be a large number of elements (spatial variations in intensity) each to some degree visible and on the whole densely and evenly arrayed over the field of view. The elements and rules of spacing or arrangement may be arbitrarily manipulated. If a sufficient amount of detail is present in a small visual angle, a characteristic texture emerges even when the elements or spacing are randomly distributed. A checkerboard, for instance, is a deterministic texture where the patterns are strictly ordered. In stochastic textures, the spatial distribution of the pattern is random. A textural

pattern may sometimes have sub patterns within itself. Such a type of textures is referred to as a micro texture.

Texture analysis techniques have been broadly categorized into three major groups. They are statistical, structural and spectral approaches. In statistical approaches, the presence of texture and the statistical parameters such as mean, standard deviation or higher order statistics, or correlation etc., computed on these texture images, are used for subsequent analysis, the various methods so far proposed for texture analysis are reviewed briefly in the following sections.

2.2 MAJOR APPROACHES IN TEXTURE ANALYSIS

2.2.1 Statistical Methods

In these methods, the statistical properties of texture images are explored for further analysis. The simplest method is to use the gray level averages derived from the pixel intensity values. These depend only on the individual pixel values, not on the interaction of pixel values in a spatial support. With first order statistics, only a limited number of textures can be discriminated. Moreover, two different classes of texture can have the same mean. There are also other methods based on the statistics of the gray levels in an image segment. They aim to understand the non-deterministic properties of the texture that govern the distribution and relationship between the gray levels of the image. Coggins and Jain (1985) have explained the spatial filtering approach to texture analysis. Recently, a review is presented for the texture analysis (Bharathi et al 2007).

2.2.1.1 Spatial gray level dependence matrix (SGLDM)

Davis et al (Davis 1979) and (Davis and Mitche 1981) describe the generalized co-occurrence matrices for texture discrimination. These do not describe the texture directly but rather describe the spatial arrangement of local image features such as edges and lines. Gonzalez et al (2002) and Julesz et al (1978) illustrated the visual discrimination of textures with identical third order statistics.

This well known technique calculates a set of features based on the co-occurrence of gray levels in pixel pairs with specified orientation to one another. Haralick et al (1973), Haralick (1979) and Gotlieb et al (1990) suggested the use of a gray level co-occurrence matrix (GLCM) for computing texture features. The relative frequencies of co-occurrence describe how frequently two pixels with gray levels (a, b) appear in the image 'f' of window size (M × N), separated by a distance 'd' in the direction ϕ. The frequencies are represented in the form of a matrix and there were fourteen features suggested to be computed. These features have been computed and are applied to a variety of texture analysis problems. The main problem in using the co-occurrence matrix method is that it has a high time complexity and the number of features are more. The selection of the direction and the distance between the co-occurring pixels are critical. That is why a subset of these fourteen features is used in solving many texture related problems.

Walker et al (Walker et al 1995) proposed an interesting method of improving the quality of co-occurrence matrix features. They classify the features proposed by Haralick et al as being weighted on either the matrix element's value or its spatial location. For example, energy and entropy measures are weighted on the basis of value, and inverse difference moment,

shade, inertia, correlation and variance are weighted on the basis of spatial location. The authors propose that it is best to suppress those elements of the matrix that yield little to the discrimination ability. Hence, on the basis of the Bhattacharya distance calculation, one can find which elements are the most discriminatory. A discrimination matrix containing these weights can be multiplied with the original matrix to yield a better representation of values that are discriminatory. Hauta-kasari et al (1996) investigated the well known co-occurrence matrix method.

2.2.1.2 Gray level run length matrix (GLRLM)

"A gray level run" is a set of consecutive, collinear picture points having the same gray level value. The length of the run is the number of picture points in the run. The runs are represented in the form of a two dimensional matrix, with gray levels as rows and the length of runs in columns. There are five features such as Long Run Emphasis, Short Run Emphasis, Run Percentage, Gray Level Non Uniformity and Run Length Non Uniformity. These five features can be computed from the run length matrix. Galloway (1975) performed a texture analysis of 54 terrain samples with run length features. The samples are taken from nine categories: orchard, wood, urban, suburb, lake, marsh, swamp, railroad and scrub. A classification accuracy of 83% has been reported. The main disadvantage of this method is its high requirement of computational time and the fact that it is noise sensitive.

2.2.1.3 Texture energy measure

Laws has proposed a 'texture energy measure' method (Laws 1979) which involves convolving the image with small masks and then computing variance like expected values over all neighborhoods. These measures

determine the textural properties by assessing average gray level, edge, spots, ripples and waves in the texture image. The average absolute values for a set of masks can be jointly used to classify textures. Laws obtained classification accuracy of over 80% in his studies (Laws 1980). Texture statistics based on gray values of an image directly, are sensitive to noise, luminance variation, contrast and other monotonic shifts of gray values. Harrwood (Harrwood et al 1985) proposed a rank correlation method to avoid this dependence. The local rank order of the gray values is used instead of the gray values themselves. These rank orderings are obviously invariant to any monotonic gray value transformations. The experimental result for the six-texture classification problem is 95 % for the rank correlation method while it is 85% for the texture energy measure method.

The vectors used to derive the measures are,

$$\begin{aligned} L_5 &= L_3 * L_3 = [1 \quad 4 \quad 6 \quad 4 \quad 1]: \textit{level} \\ S_5 &= E_3 * E_3 = [-1 \quad 0 \quad 2 \quad 0 \quad -1]: \textit{spot} \\ R_5 &= S_3 * S_3 = [1 \quad -4 \quad 6 \quad -4 \quad 1]: \textit{ripple} \\ E_5 &= L_3 * E_3 = [-1 \quad -2 \quad 0 \quad 2 \quad 1]: \textit{edge} \\ W_5 &= E_3 * S_3 = [-1 \quad 2 \quad 0 \quad -2 \quad 1]: \textit{wave} \end{aligned} \tag{2.1}$$

Using the above five 1×5 vectors, Laws 5×5 masks are generated,

$$L_5^T \times S_5 = \begin{bmatrix} -1 & 0 & 2 & 0 & -1 \\ -4 & 0 & 8 & 0 & -4 \\ -6 & 0 & 12 & 0 & -6 \\ -4 & 0 & 8 & 0 & -4 \\ -1 & 0 & 2 & 0 & -1 \end{bmatrix} \tag{2.2}$$

The texture samples are first convolved with one of the masks. Then a measure of the ‘local texture energy’ is computed which is the average

absolute value of convolutions across all neighborhoods. The average absolute values for a set of masks can be jointly used to classify textures. Laws obtained classification rates of over 80% in his studies.

2.2.1.4 Moments

Tucceryan (1992) used moments of an image to compute texture features. The $(p+q)^{th}$ order moments of the image function f(x, y) with respect to origin are defined as,

$$m_{pq} = \int_{-\infty}^{\infty}\int_{-\infty}^{\infty} x^p\, y^q\, f(x,y)\, dx\, dy \tag{2.3}$$

The moments are normally computed over some bounded region R. The moments $m_{00,}$ m_{10}, m_{01}, m_{20}, m_{11} and m_{02} are computed for each pixel over a small local window around that pixel, resulting in six moment images namely m_1, m_2, m_3, m_4, m_5 and m_6. The feature image $F_k(i, j)$ is obtained by transforming the moment image m_k with mean $\overline{m}$ using the hyperbolic tangent function Tucceryan (1992),

$$F_k(i,\ j) = \frac{1}{L^2} \sum_{(a,b)\in w_{i,j}} \left|\ \tanh\ \left[\sigma\left(m_k(a,b) - \overline{m}\right)\right]\ \right| \tag{2.4}$$

where w_{ij} is an L×L averaging window centered at location (i, j). The shape of the logistic function is controlled by 'σ'. Then, for a pixel at (i, j), a textural feature vector (T_{ij} = <F_1(i,j)…F_n(i,j)>) is defined. Texture segmentation is performed by applying a general purpose clustering algorithm to the feature T_{ij}. Though this algorithm successfully segments binary textures and a

number of gray level textures, there is no study on the impact of window size and the number of moments, on the segmentation performance.

Coroyer Lacos et al (1997) presented a texture classification scheme based on higher order statistics, such as bi-correlation in the spatial domain, and the bi-spectrum in the frequency domain.

2.2.1.5 Neighborhood gray tone difference matrix (NGTDM)

Amadasun and King (1989) proposed the NGTDM in an attempt to define texture measures correlated with the human perception of textures. The matrix is a column vector and the elements are computed based on measuring the difference between the intensity level of a pixel and the average intensity over a square, sliding window centered at the pixel. For an image (M×N) size with 'G' number of gray levels, the computation is as follows. The average intensity over a window of size (k × k) is,

$$f_i = \frac{1}{w - 1} \sum_{m=-k}^{k} \sum_{n=-k}^{k} f(x + m, y + n) \qquad (2.5)$$

where $w = (2k+1)^2$. The i^{th} entry of the NGTDM is

$$S(i) = \sum_{x=0}^{M-1} \sum_{y=0}^{N-1} |i - f_i| \qquad (2.6)$$

for all pixels having intensity level 'i'. Five different features are derived from NGTDM as follows:

1. Coarseness, which is defined by the size of the texture primitives,

$$C_{\cos} = \left[\varepsilon + \sum_{i=0}^{G-1} p_i \quad S \right. \tag{2.7}$$

where 'ε' is a small number to prevent the coarseness coefficient becoming infinite and $p_i = N_i / n$ is the estimated probability of the occurrence of the intensity level 'i', with N_i denoting the number of pixels having an intensity 'i' and n = (N-k)(M-k).

2. Contrast, which depends on the intensity difference between neighboring pixels,

$$C_{con} = \left[\sum_{i=0}^{G-1} \sum_{j=0}^{G-1} p_i \, p_j \, (i - j)^2 \right] \left[\frac{1}{n} \sum_{i=0}^{G} S(i) \right] \tag{2.8}$$

3. Busyness, described by high spatial frequency of intensity changes,

$$C_{bus} = \frac{\sum_{i=0}^{G-1} p_i S_i}{\sum_{i=0}^{G-1} \sum_{j=0}^{G-1} \left| i \, p_i - j \, p_j \right|}, \quad p_i \neq 0, \quad p_j \neq 0 \tag{2.9}$$

4. Complexity, which depends on the number of different primitives and different average intensities,

$$C_{com} = \sum_{i=0}^{G-1} \sum_{j=0}^{G-1} \frac{|i-j|}{n(p_i + p_j)} \left[p_i S(i) + p_j S(j) \right], \quad p_i \neq 0, p_j \neq 0 \tag{2.10}$$

5. Texture strength, which indicates clearly definable and visible primitives,

$$C_{str}=\frac{\sum_{i=0}^{G-1}\sum_{j=0}^{G-1}(p_i+p_j)(i-j)^2}{\varepsilon+\sum_{i=0}^{G-1}S(i)}, \qquad p_i\neq 0, p_j\neq 0 \tag{2.11}$$

Using the above five features, Christodoulou et al (2003) have performed classification experiments and reported 54.1 % accuracy.

2.2.1.6 Histogram measures

The most common class of texture features is the following measures (Unser 1986), computed from the histogram of the image under analysis.

$$mean\ \ \mu=\frac{\sum_{i,j}x_{ij}}{n} \tag{2.12}$$

$$mean\ \ Euclidean\ \ disance\ =\ \frac{\sqrt{\sum_{i,j}\left(x_{ij}-x_i\right)^2}}{n-1} \tag{2.13}$$

$$Variance\ \sigma^2\ =\frac{\sum_{i,j}\left(x_{ij}-\mu\right)^2}{n-1} \tag{2.14}$$

$$Skew\ \ =\ \ \frac{\sum_{i,j}\left(x_{ij}\ -\ \mu\right)^3}{(n\ -\ 1)\sigma^3} \tag{2.15}$$

$$kurtosis \quad = \frac{\sum_{i,j} \left(x_{ij} - \mu \right)^4}{\left(n - 1 \right) \sigma^4} \tag{2.16}$$

$$entropy \quad H = -\sum p_{ij} \log p_{ij}$$

$$with \quad p_{ij} = \frac{x_{ij}}{\sum_{i,j} x_{ij}} \tag{2.17}$$

$$energy \, E = \sum_{i,j} x_{ij}^2 \tag{2.18}$$

where x_{ij} stands for the pixel value at (i, j), 'n' is the number of pixels and x_i is the window's center pixel value.

The spectral histogram consists of marginal distribution of responses of a bank of filters and encodes implicitly the characteristic structure of images through the filtering stage and the global appearance through the histogram stage. The distance between spectral histograms is measured using the chi-square statistic. The spectral histogram with the associated distance measure exhibits several properties that are necessary for texture classification. A filter classification algorithm is proposed to maximize the classification performance of a given data set. The classification experiments using natural texture images reveal that the spectral histogram representation provides a robust feature statistic for textures (Xiuwen Liu and Deliang Wang 2003).

2.2.2 Structural Methods

On the structural level, a texture is considered to be defined by elements, which occur repeatedly according to some placement rules. In the

bottom-up analysis procedure, the texture primitives are extracted; later the spatial arrangement or the placement rules of the elements is studied. These methods often become sensitive to various degradations of the images. The top-down methods in which the spatial structure of texture is recognized before the element extraction. Also it has been reported that edge-based schemes for primitive extraction yield better results than threshold-based schemes (Hong et al 1980). Description of textures by a structural analysis has been discussed in (Tomita et al 1982).

Tsuji and Tomita (1973) performed by experiment in which the unit patterns or atomic regions were found by a simple thresholding method. The measures used to characterize the unit patterns were the central moments m_{20}, m_{02}, m_{21} and $m_{11.}$ The placement rules for the various unit patterns were measured by a density descriptor. An atomic region 'A', in a given set 'S' has a density descriptor D_s, whose value is the minimum distance from 'A' to other atomic regions in 'S'. This simple procedure is limited to a few textures which it can handle.

Zucker et al (1975) considered various sizes of "spot" unit patterns and found them using a spot detector. No measures were extracted to characterize these spot patterns. Rather, only the number of spots of various sizes present in the texture was recorded. The method had no mechanism to characterize the placement rules of the spots. This severely limits the generality of this approach. In another method (Ehrich et al 1978), the unit patterns considered are regions centered about a local maximum, bounded on all sides by local minima. The unit patterns are referred to as "peaks". The measures used to characterize the peaks are absolute peak height, relative peak height and the area of the region where the peak is located. This method also lacks in characterizing the placement rules.

Conners and Harlow (1980) used the statistical texture measures, spatial gray level dependence matrix (SGLDM) in developing a structural textural analyzer. This method is based on searching the unit pattern, which is a period parallelogram. Periodicity vectors are found as displacement vectors of the co-occurrence matrices with the smallest moment of inertia. It has been shown that the SGLDM feature, inertia measure is effective in characterizing both the unit pattern and the placement rules.

Voorhees and Poggio (1987) suggested a method based on filtering the texture image with Laplacian of Gaussian (LoG) masks at different scales and combining this information to extract blobs in the image which are important in texture perception. Tuceryan and Jain (1990) proposed the extraction of texture features by using the properties of the Voronoi tessellation of the given image. Considering an arbitrary pair of points 'p' and 'q', the bisector of the line joining 'p' and 'q' is the locus of the points equidistant from both 'p' and 'q' dividing the plane into two halves. The half plane $H_P^q(H_q^p)$ is the locus of points closer to p(q) than to q(p). For any given point 'p', a set of such half planes is obtained for various 'q'. The intersection of H_{Pq} defines a polygon region consisting of points closer to 'p' than to any other point. Such a region is called the Voronoi diagram. The Voronoi diagram with the incomplete polygons in the convex hull defines a Voronoi tessellation of the entire plane. Moments of area of the Voronoi polygons serve as a useful set of features that reflect both the spatial distribution and shapes of the texture tokens in the image. The authors extracted five features,

$$f_1 = m_{00} \tag{2.19}$$

$$f_2 = \sqrt{\bar{x}^2 + \bar{y}^2} \tag{2.20}$$

$$f_3 = \tan^{-1}\left(\frac{\bar{y}}{\bar{x}}\right) \tag{2.21}$$

$$f_4 = \frac{\sqrt{\left(m_{20} - m_{02}\right)^2 + 4m^2_{11}}}{m_{20} + m_{02} + \sqrt{\left(m_{20} - m_{02}\right)^2 + 4m^2_{11}}} \tag{2.22}$$

$$f_5 = \tan^{-1}\left(\frac{2m_{11}}{m_{20} - m_{02}}\right) \tag{2.23}$$

where $(\bar{x}, \bar{y})$ are the coordinates of the Voronoi polygon's centroid. These features have been used for a segmentation of textured images.

Davis (1979) concentrated on describing the spatial structure of dot patterns in an image. Since all the texture elements (dot pattern) have identical properties, the spatial arrangement of the dot patterns is the only distinguishing feature. Therefore, a histogram of directions between a point and its 'k' nearest neighbors is constructed. Sharp peaks are detectable in the histogram for regular textures and the distribution is uniform for random point patterns.

Some of the other most popular texture feature extraction methods are based on the gray level texton gradients, edge gradients (Marr 1980), filtering methods like morphological filters, Fourier filters, Random Field Models (Chellappa 1985), Gabor filters (Fogel 1989), (Grigorescu 2002) Wavelet Packet approaches (Chang 1993; Laine and Fan 1993), Wavelet Frames (Unser 1995), Wavelets like Gaussian (Cheriet 1998; Charalampidis 2002), fractal dimension (Kaplan 1999), and Local binary patterns (Ojala et al 2002). Each method is good in discriminating the texture of its characteristics and there is no unique method available for detecting all textures. In the study

conducted by Randen et al (Randen et al 1999) it is observed that the particular texture classification technique is restricted to a limited real texture. Every texture has a band of frequency components in it where the selection of filter banks for extracting the features becomes a non-trivial task.

Kulkarni et al (Kulkarni 2002) proposed and investigated an auto-associator texture feature extractor and two hybrid intelligent techniques such as an auto-associator-Multi Layer Perceptron (MLP), and statistical-MLP for texture feature extraction and classification. They showed that the auto-associator is capable of separating texture classes very well and without any feedback from the user. The feature extraction and classification techniques were tested on a large database of texture patterns namely the Brodatz texture database. The results obtained were analyzed and compared with other intelligent and conventional techniques.

2.2.3 Spectral Methods

A method for texture analysis using the Fourier spectrum has been proposed by Bajcsy 1976, Dyer 1976 and Weszka 1976. The Fourier transform of an image f(x,y) is designed as

$$F(u,v) = \iint e^{-2\,i(ux + vy)} f(x,y)\, dx\, dy \qquad (2.24)$$

and the Fourier power spectrum is $|F|^2 = FF^*$, (where * denotes the complex conjugate). The radial distribution of values in $|F|^2$ is sensitive to texture coarseness in F. A coarse texture will have high values of $|F|^2$ concentered near the origin, while in a fine texture the values will be more spread out. Thus, if one wishes to analyze texture coarseness, a set of features that should be useful are the average of $|F|^2$ taken over ring-shaped regions centered at the origin. Similarly the angular distribution of values in $|F|^2$ is sensitive to

the directionality of the texture in f. A texture with many edges or lines in a given direction θ will have high values of $|F|^2$ concerted around the perpendicular direction θ= Π/ 2 while in a non-directional texture $|F|^2$ should also be non directional. Thus a good set of features for analyzing the directionality of texture may be obtained based on average values of $|F|^2$ taken over wedge – shaped regions centering at the origin. When textured features based on the discrete Fourier power spectrum are used for pattern classification, the performance has been found to be poor (Dyer 1976) due to the presence of aperture effects in the spectrum. This is because of the fact that the Discrete Fourier Transform treats the given image as if it is always periodic.

Spectral techniques for texture segmentation typically use the power spectrum of a region than its amplitude spectrum. Radial or angular integration of the power is often performed. Radial integration sums power within a ring of radius r and width Δr. Angular integration sums power within a sector defined by radius, an orientation θ, and an angular width Δθ. The ring based measurement provides information on the scale of the texture, high power at small radii signifies coarse texture, whereas a concentration of power at large radii indicates fine texture. The sector based measurement provides information on the orientation of the texture; a texture that is oriented in a direction indicated by an angle φ will result in high power for a sector at angle θ = φ + Π / 2 (Nick Effort 2004). i.e, The degree of texture coarseness is proportional to its spatial period. Thus a region of coarse texture should have its Fourier spectral energy concentrated at low-spectral frequencies. Conversely, regions of fine texture should exhibit a concentration of spectral energy at high spatial frequencies. Although, this correspondence exists, to some degree, difficulties often arise because of spatial changes in the period and the phase of the texture pattern repetitions (Joshi 2006).

2.2.4 Model Based Methods

So far the features computed either directly from the texture image or from the intermediate representation, such as co-occurrence or run length matrix are described. In this section, a few mathematical model-based approaches and their usages are described. In model-based methods, texture images are considered as samples of spatial random fields. The models assume some kind of dependence a pixel has on its neighborhood. This can be a linear dependence as with autoregressive models or a joint probability as with Markov fields. Texture features are derived by fitting the random fields to image data. The model parameters capture the essential perceived qualities of texture. These models can be used not only to describe texture, but also to synthesize it. A model based method for rotation invariant texture classification is illustrated (Kashyap and Khotanzd 2001).

2.2.4.1 Auto regressive model

The autoregressive (AR) model assumes a local interaction between image pixels as a weighted sum of neighboring pixel intensities. Assuming the image ‘f’ to be a zero mean random field, an AR causal model can be defined as,

$$f_s = \sum_{r \in N_S} \theta_r f_r + e_s \tag{2.25}$$

where f_s is image intensity at site ‘s’, ‘e_s’ denotes an independent and identically distributed noise, N_s is a neighborhood of ‘s’ and ‘θ’ is a vector of model parameters. In the case of a simple pixel neighborhood that comprises ‘n’ immediate pixel neighbors, there are (n+1) unknown model parameters. They are the standard deviation ‘σ’ and model parameter vector

$\theta = (\theta_{1,}\theta_{2...}\theta n)$. By minimizing the sum of squared error, the parameters can be estimated through the following equations,

$$\sum_s e_s^2 = \sum_s \left(f_s - \hat{\theta} w_s \right)^2 \tag{2.26}$$

$$\hat{\theta} = \left[\sum_s w_s w_s^T \right]^{-1} \left[\sum_s w_s f_s \right] \tag{2.27}$$

$$\sigma^2 = N^{-2} \sum_s \left(f_s - \hat{\theta} w_s \right)^2 \tag{2.28}$$

where, $w_s = \text{col}\,(f_i,\ i \in N_s)$ for a square image of N×N size. The obtained model parameter values are used for texture description (Sarkar et al 1997). Texture classification and segmentation using multi resolution simultaneous auto regressive models has been successfully attempted by Mao and Jain (1992).

2.2.4.2 Markov random field (MRF) model

A Markov random field is a probabilistic process in which all interactions are local. The probability that a point is in a given state is entirely determined by the probabilities of the states of neighboring points. A discrete 2D random field, defined over a finite $N_1 \times N_2$ rectangular lattice of points (corresponding to pixels in digital image) is defined as,

$$L = \{ (i, j) : 1 \le i \le N_1,\ 1 \le j \le N_2 \} \tag{2.29}$$

$$\eta = \{ \eta_{ij} : (i, j \in L,\ \eta_{ij} \in L) \} \tag{2.30}$$

A collection of subsets of L described as, is a neighborhood system on L if and only if η_{ij}, the neighborhood of pixel (i, j) is such that,

$$1.\ (i,\ j) \notin \eta_{i\ j}$$
$$2.\ if\ \ (k,l) \in \eta_{i\ j},\ then\ (i,\ j) \in \eta_{k\ l}\ \ for\ \ any\ (i,\ j) \in L \tag{2.31}$$

A random field X={X_{ij}} defined over lattice L is a Markov Random field (MRF) with respect to the neighborhood system 'η' if and only if,

$$P\left(X_{ij} = x_{ij} \middle|\ X_{kl} = x_{kl},\ (k,l) \in L,\ (k,l) \neq (i,j) \right) \tag{2.32}$$

$$\begin{aligned} &= P\left(X_{ij} = x_{ij} \middle|\ X_{kl} = x_{kl}, (k,l) \in \eta_{ij} \right) \\ &for all (i,j) \in L\ and\ P(X = x) > 0\ for all\ x \end{aligned} \tag{2.33}$$

The problems of texture analysis have been investigated using the Markov random fields in (Gross and Jain 1983; Krishnamachari and Chellappa 1997; Andrey and Darrox 1998).

2.2.4.3 Fractal model

Fractals are effective in modeling the statistical quality of surface roughness and self-similarity at different scales. The fractal dimension 'D' gives a measure of the roughness of the surface. The larger the value of 'D', the rougher the texture is. Therefore, fractal dimension can be a texture feature for discrimination purposes. The fractal dimension can be estimated from an image as proposed by Voss 1986. P(m, L) is the probability that there are 'm' points within a box of side length 'L' centered at an arbitrary point on the image surface 'A'. 'M' is the total number of points in the image.

When the image is overlaid with boxes of length 'L', then (M/m) P(m,L) is the expected number of boxes with 'm' points inside. The expected total number of boxes needed to cover the whole image is,

$$E(N(L)) = M \sum_{m=1}^{N} \left(1/m\right) P(m, L)$$

The expected value of N(L) is proportional to L^{-D}. This can be used to estimate the fractal dimension 'D'.

Perceptually different textures may have similar fractal dimension. Therefore, another measure, called 'Lacunarity" has been suggested to compensate the inadequacy of fractal dimension 'D' [Keller et al 1989]. Lacunarity 'Λ' is defined as,

$$\Lambda(L) = \frac{m^2(L) - \left[m(L)\right]^2}{\left[m(L)\right]^2} \tag{2.24}$$

where

$$m(L) = \sum_{m=1}^{N} m\, P(m, L) \tag{2.25}$$

$$m^2(L) = \sum_{m=1}^{N} m^2\, P(m, L) \tag{2.26}$$

and P(m,L) is the probability distribution.

2.2.5 Transform Methods

The human visual system, as evidenced by much psychophysical and neuro physiological data, performs some form of local spatial-

frequency analysis on the retinal image and this analysis is done by a bank of tuned band pass filters (Beck et al 1987) and (Kube and Pentland 1998). This inspired researchers to design individual filters and the configuration of the filter bank. Several classes of functions such as Gabor elementary functions, a difference of offset Gaussian, Gaussian derivatives and wavelet functions have been proposed for the filters. These filters decompose a textured image into a joint space/spatial-frequency representation and the filter outputs are characteristic signatures for performing texture analysis.

2.2.5.1 Spatial filters

Edge density per unit area can be a texture measure. Fine textures tend to have a higher density of edges per unit area than coarse textures. Simple edge masks such as the Roberts operator (Roberts 1982) or the Laplacian operator (Sonka et al 1999) given below compute the measurement of edge ness.

$$m_1 = \begin{bmatrix} 1 & 0 \\ 0 & -1 \end{bmatrix} \quad m_2 = \begin{bmatrix} 0 & 1 \\ -1 & 0 \end{bmatrix} \qquad L = \begin{bmatrix} -1 & -1 & -1 \\ -1 & 8 & -1 \\ -1 & -1 & -1 \end{bmatrix} \tag{2.27}$$

Roberts operator *Laplacian operator*

The magnitude of the responses of these masks over an image area may be treated as a texture measure. Malik and Perona (1990) proposed a spatial filtering approach which had three stages: i) convolution of the image with a bank of even-symmetric filters using differences of offset Gaussian (DOOG) functions, followed by half wave rectification, ii) inhibition of spurious responses in a localized area and iii) detection of boundaries between different textures, by applying edge detection methods on the feature images obtained in the previous stage. It has been demonstrated that this method is

able to discriminate natural as well as synthetic textures. Bovik et al (1990) illustrated the concept of multi channel texture analysis using localized spatial filters.

2.2.5.2 Gabor filters

In a joint space / spatial-frequency representation for images, frequency is viewed as a local phenomenon (i.e.,as a local frequency) that can vary with position throughout the image. Then, the texture segmentation problem is to locate regions of similar local spatial-frequency content. Dunn et al (1994) performed texture segmentation with Gabor filters and provided detailed criteria for designing individual filters. The filter operation is expressed as,

$$m(x,y) = |f(x,y) * h(x,y)| \tag{2.38}$$

where* denotes convolution, f(x, y) is an image function and 'h' is the Gabor elementary function (GEF) and m(x, y) is the filter output. GEF which is also referred to as the Gabor wavelet is a Gaussian modulated by a complex sinusoid,

$$h(x,y) = g(x',y') \exp\left[j2\pi \left(U_x + V_y\right)\right] \tag{2.39}$$

where (x′,y′) = (xcosθ +ysinθ, - xsinθ+ycosθ) are rotated spatial-domain rectilinear co-ordinates, and (U,V) represents particular 2D frequency of the complex sinusoid.

$\phi=\tan^{-1}$ (V/U) specifies the orientation of the sinusoid, g(x, y) is the 2D Gaussian as given by,

$$g(x,y)=\frac{1}{2\pi\sigma_x\sigma_y}\exp\left\{-1/2\left[\left(\frac{x}{\sigma_x}\right)^2+\left(\frac{y}{\sigma_y}\right)^2\right]\right\} \quad (2.40)$$

and (σ_x, σ_y) characterize the spatial extent and bandwidth of 'h'. The aspect ratio of g(x, y) is given by $\lambda = (\sigma_y/\sigma_x)$ which is a measure of the filter's asymmetry. GEFs are band pass filters and can be configured to extract a specific band of frequency components from an image. The Gabor filter output for characteristic signatures such as step, ridge, valley or step changes in average local output variations have been analyzed. These signatures depend on the type of texture differences across the boundary in a composite image.

Azencott et al (1997) used Gabor filters with an aspect ratio 'λ' equal to one and σ=4 pixels. The spatial frequencies, which constitute the discrimination of the spatial frequency domain, are taken as uniformly distributed in four orientations (θ, π/4, π/2, 3π/4). Kullback distance between the textures based on the spectral densities is,

$$D(f,f')=\frac{1}{\sum_{(\theta,r)\in T'} r}\sum_{(\theta,r)\in T'} r\left[\frac{f(\theta,r)}{f'(\theta,r)}+\frac{f'(\theta,r)}{f(\theta,r)}-2\right] \quad (2.41)$$

where, f(θ, r) and f′(θ, r) are the spectral density estimates of textures X and Y computed using the filters, and T′ is a set which corresponds to uniform discretizations in orientation (θ) and modulus(r). The result of the classification with Kullback distance is around 97% and, with quadratic distance, it is around 90%. A comparison of texture features based on Gabor filters have been presented in Grigorescu et al 2002. Analysis of multi

channel narrow band filters for image texture segmentation has been presented in Bovik 1991.

2.2.5.3 Wavelet filters

A multi-resolution representation provides a simple hierarchical framework for interpreting image information. At different resolutions, the details of an image generally characterize different physical structures of the scene. At coarse resolution, the details correspond to the larger structures, which provide the image "context". It is therefore natural to analyze first the image details at a coarse resolution and then gradually increase the resolution. The wavelet decomposition of a signal f(x) is performed by a convolution of the signal with a family of basis functions 'ψ' ,

$$\left\langle f(x)\, \psi_{2^s,t}(x) \right\rangle = \int_{-\infty}^{\infty} f(x)\, \psi_{2^s,t}(x)\, dx \qquad (2.42)$$

where 's', 't' are referred to as the translation and dilation parameters respectively. In the case of two-dimensional images, the wavelet decomposition is obtained with separable filtering along the rows and along the columns of the image (Mallat 1989). Level 1 and level 2 image decomposition are illustrated in Figure 2.1.

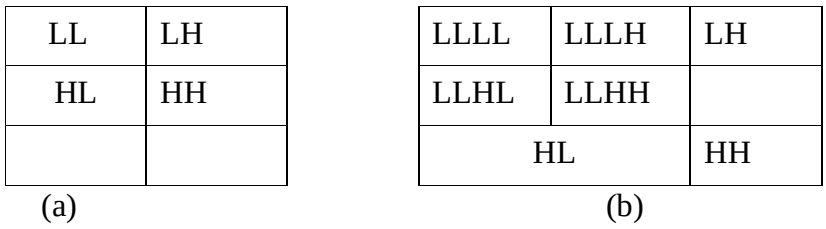

Figure 2.1 Wavelet decomposition (a) Level 1 decomposition (b) Level 2 decomposition (b) Level 2 decomposition

The wavelet analysis can thus be interpreted as image decomposition in a set of independent, spatially oriented frequency channels. The HH sub image represents diagonal details i.e., high frequencies in both directions i.e. the corners. HL gives horizontal edges and the image LL corresponds to the lowest frequencies. Each stage of analysis produces the next 4 sub images whose size is reduced twice compared to the previous scale.

Mallat (1989) expressed the similarity between Julez's "theory of textons" (Julesz 1981) and the wavelet theory. Julesz has developed a texture discrimination method based on the decomposition of textures into basic primitives called textons. These textons are spatially local and they have a particular spatial orientation and narrow frequency tuning. The wavelet representation can also be interpreted as a texton decomposition where each texton is equivalent to a particular function of the wavelet ortho-normal basis. Three level decomposition was used in (Porter et al 1996) resulting in 10 main wavelet channels. The energy of each channel can be evaluated by simply calculating the mean magnitude of its wavelet coefficients,

$$C_n = \frac{1}{MN} \sum_{x=0}^{M-1} \sum_{y=0}^{N-1} \left| w(x, y) \right| \tag{2.43}$$

where the channel is of dimension M by N and w(x, y) is a wavelet coefficient within a channel. The image is first split into smooth and textured regions based on the value of the following parameter,

$$R = \frac{C_1 + C_2 + C_3 + C_4}{C_5 + C_6 + C_7} \tag{2.44}$$

The region is labeled smooth if R>=T or textured if R<T where T is the threshold. Appropriate features are then selected for the regions, to perform segmentation.

It is a challenging task to select the most important features in a set so as to reduce the feature vector length and at the same time to retain as much as possible their class discriminatory information. Sabri et al (2003) proposed local discriminant basis (LDB) algorithm to achieve this. LDB is based on wavelet transform, so that it can effectively represent a non-stationary signal with a few numbers of significant coefficients. Wavelet packet transform is a generalization of discrete wavelet transform, which can be implemented by means of quad tree structure of low pass and high pass quadrate mirror filters. The best path or best basis on the tree is iteratively found out by imposing an additive discriminant measure as a criterion. The selected basis functions are ordered based on their discrimination power. The 'k' most discriminant basis functions are used for constructing the classifier. LDB has been shown to be capable of 85% accurate classification of textured images using only the top 280 LDB features.

Fourier transforms lack spatial localization whereas the Gabor transform has no single filter resolution at which spatial localization is represented. Wavelet transforms are effective in representing textures at the most suitable scale (Lu et al 1997). An application for analyzing mammograms using the concept designed for using wavelets for target detection has been illustrated in Boccignone et al (2000).

2.3 TEXTURE CLASSIFICATION

Texture classification work has been attempted by various researchers as applications of their proposal for texture representation. This

section reviews briefly the various schemes suggested for texture classification. Texture classification is measured based on the correct classification against misclassification. Various techniques have been discussed by Chen (1995). Hamdan and Larson (2002) illustrated the use of level lines for the texture classification, two stage wavelet based technique by Pan and Lee (2001). Structural approach to identify the defects in textured images is explained in (Chen and Jain 1990].

A simplex-Genetic hybrid approach for the classification of texture images has been attempted by Li Pan and Hong Zheng (2005). The simplex method is a kind of local searching method that gets new and better simplex points by reflection, expansion and contraction operations. Since the method converges quickly, they employed the local search characteristic of the simplex method to avoid the pre-mature of genetic algorithms. Based on the integration of genetic algorithms and the simplex method, a hybrid algorithm is proposed, to discriminate image textures. They used aerial images for the classification experiments. Various statistical geometrical features for texture classification has been presented (Chen; Nixon and Thomas 1995).

Support vector machines (SVM) and the wavelet transform have been successfully combined for performing texture analysis and used for classification (Samsher Sidhu and Raahemifar 2005). The choice of the mother wavelet determines the classification results in the case of a wavelet-based texture analysis. The use of the mother wavelet filters in a probabilistic approach to texture analysis is based on adaptive bi-orthogonal wavelet packet bases. The optimal choice for the mother wavelet filters is estimated from the data, in addition to the other model parameters (Abhayaratne and Zerubia 2005). A new model for image texture classification is also suggested, based on wavelet transformation and SVD (Ramakrishnan and Selvan 2006) and (Selvan and Ramakrishnan 2007). A Support vector

machine which employs a kernel corresponding to feature extraction of local higher order moment spectra (LHOMS) of an image is introduced. In order to overcome the dimensionality, when utilizing LHOMS image features in conventional multi channel filtering, an inner product kernel is derived. In the experiments, the SVM with LHOMS kernel is applied to image texture classification (Keisuke Kameyama and Kei Taga 2004).

A novel approach based on Artificial Crawlers for texture classification has been presented (Duo Zhang and Chen 2004). A model of artificial organisms, i.e. Artificial Crawlers and a series of evolution curves represent the features of the texture. The distributed ACrawlers interact locally with their living environment, i.e. textured regions and each ACrawler acts according to a set of homogeneous rules for isotropic motion, energy absorption, colony formation etc. The properties of the individual ACrawler and the artificial life model for texture classification have been discussed.

The features based on MRF models are usually sensitive to the rotation of image textures. An isotropic circular Gaussian MRF model is used for modeling rotated image textures and retrieving rotation invariant texture features. These features are used for classifying SAR (Synthetic Aperture Radar) sea ice and Brodatz imagery (Deng and Clausi 2003). The Gauss-MRF parameters allow the characterization of different hyper spectral (images with fine spectral and spatial sampling) textures. Using this approach, the urban areas are classified in their experimentation (Rallier et al 2004). Total variation is used to suppress the instability of least square error instead of the regularization technique for texture classification in remotely sensed images (Wang et al 2003) and claimed to be good for remotely sensed images. Forest structure classification using Airborne Multi spectral image texture and Kriging analysis has been presented by Zhang and Franklin 2002. The classification of satellite cloud imagery, based on multi-feature texture

analysis and neural networks is presented in Christodoulou et al 2001. An unsupervised classification algorithm is derived by modeling observed data as a mixture of several mutually exclusive classes that are each described by linear combination of independent, non Gaussian densities (Te-Won Lee and Lewicki 2002). A system has been developed based on multi feature texture analysis and modular neural networks that will facilitate the automated interpretation of satellite cloud images. They have classified 366 cloud segments into six texture classes using geostationary METEOSAT7 satellite images, and used them for further processing (Christodoulou et al 2003). The research into satellite cloud image recognition based on variational method and texture feature analysis is presented in (Wei Shangguan et al 2007). The research aspect concentrates on how to judge the cloud type and classify the cloud mainly.

The textural information of a multi-temporal set of ERS-1 and JERS-1 AR images was studied with the first and second order statistical measures. These measures had a higher information value for the land-cover and forest type classification than the SAR image intensity. The multi-spectral approach was beneficial for the application of the textural measures. The textural parameters significantly improved the classification of land cover and forest types (Lauri Kurvonen and Martti T. Hallikainen 1999).

A new scheme of fusing cortex transform and brightness features obtained by local windowing operations is proposed. Three brightness-based features are obtained and their correlation in feature space is effectively used for texture classification with the minimum distance classifier (Bashar and Ohnishi 2002).

A linear compositional model for analyzing and classifying image textures has been presented by Huang and Chan 2002. In this model, an image

texture is considered to be a linear composition of both structural and random components. An image texture can be decomposed into two orthogonal fields, namely, the deterministic and in-deterministic fields. These two components are individually represented by using the multi channel filtering model with the Gabor wavelet and the Gaussian MRF model respectively. The composition ratio of the two components is used for the representation and classification of the textures. Rotation invariant texture classification using even symmetric Gabor filters as bee attempted by Manthalkar et al (2003).

In many popular texture analysis methods, second or higher order statistics on the relation between gray level values are stored in matrices. A high dimensional vector of predefined, non-adaptive features is then extracted from these matrices. Identifying a few consistently valuable features is important, as it improves classification reliability and enhances the understanding of the phenomena that are modeled. In a unified approach to statistical texture feature extraction, the class distance and class difference matrices are used to obtain low dimensional adaptive feature vectors for texture classification. This approach was applied to four relevant texture analysis methods. The new adaptive features outperformed the classical features when applied to the most difficult set of forty five Brodatz texture pairs (Birgitte Nielsen et al 2004).

2.4 TEXTURE SEGMENTATION

Texture segmentation is one of the very important texture analysis problems. Texture segmentation is achieved by computing the similarity or dissimilarity of the texture features. The region oriented or edge-based approaches are used for this problem. The edge-based segmentation becomes so popular as there are a number of schemes available. The conventional edge detection methods are not comfortably applied for solving the texture

segmentation problem because of the sensitivity of these methods on local micro edges. Separate edge detection or segmentation schemes are suggested in literature. Some of the significant literatures are reviewed in this section.

The usefulness of multi-channel filtering for image texture segmentation has been demonstrated in several papers. Based on psychophysical studies, it has been largely believed that Gabor filters are optimal for segmentation. The application of maximally decimated, non-separable, perfect reconstruction filter banks (sub band systems) is used for texture segmentation (Dhiraj Kacker et al 1996). In their paper, they used the sub band decomposition form, a maximally decimated filter bank and therefore they claimed that computation time and tome complexity is less. The directional selectivity achieved by the non- separable, multi rate filter bank results in a performance similar to that achievable with the Gabor filters, but with a drastically reduced computational load.

An approach for automatic video scene segmentation and content-based indexing is presented by Keesook J. Han and Ahmed H. Tewfik 1997. Scene segmentation and video indexing are based on a temporally windowed principal component-based analysis of a sub-sampled version of the video sequence. Two discriminants are derived from the principal components on a frame-by-frame basis. The discriminants are used for scene change detection and key frame extraction and classification into relevant clips. The system creates an adjacency matrix to build the scene transition graph which allows easy access to video image-based information. Other few applications can be referred from (Manjoux and Rudant 1991), (Miller and Astley 1992) and (Blostei and Ahuja 1989).

Texture analysis and segmentation of images using fractals has been successfully attempted by Fazel-Rezai and Kinsner (1999). The

objective in their paper is to decompose an image into texturally homogeneous regions using fractal dimension. Another approach for texture feature extraction is proposed by Kontaxakis et al 2003, appropriate for unsupervised texture segmentation applications. The pixel features are obtained by using the directional filters to analyze the given images to a set of sub-images, each one containing an isolated angular section of the initial image spectrum, and estimating the pixel local energy in them. By incorporating the proposed feature extraction technique into a single multi-component texture segmentation procedure, some experiments with texture separation have been implemented and the effectiveness of the presented method has been tested. The results are presented and a comparison with feature extraction techniques, based on the discrete wavelet decomposition of the image is made.

Feature fusion for image texture segmentation has been successfully attempted by David A. Clausi and Huawu Deng 2004. A design-based method to fuse Gabor filter and Gray level co-occurrence probability features for improved texture segmentation is presented. Feature space separability and unsupervised image segmentation are used for testing. The fused features are robust with respect to the curse of dimensionality and the additive noise. Feature reduction methods are typically detrimental to segmentation performance. In short, the fused features are a definite improvement over non-fused features and are advocated for texture analysis applications.

In the work reported by Assia Kourgli and Aichouche Belhadj-Aissa 2004, a novel method of optimizing the texture primitives description and segmentation using variography. The ‘variogram’ is essentially a ‘variance of differences’ in the values as a function of the separation distance. This variance therefore changes as the separation distance increases where

repetitive structures as described as hole effects. The local minima is used to find the size, shape an orientation of the unit pattern of image textures and thus to determine the optimal structuring element which is used in mathematical morphological texture analysis. The texture segmentation has been performed using the variogram characteristics. Hsiao and Sawchuk (1989) performed supervised texture segmentation using feature smoothing and probabilistic relaxation techniques. Grating cell operator features for oriented texture segmentation is achiened by Kruizinga and Petkov (1998) whereas unsupervised image segmentation using histogram clustering is discussed in Puzicha et al (1999). Texture feature performance for image segmentation is done (Du Buf et al 1990).

The Hidden Markov Tree (HMT) based image texture segmentation algorithm is presented by Hyeokho Choi and Richard G. Baraniuk 2001. HMT is a tree-structured probabilistic graph that captures the statistical properties of the coefficients of the wavelet transform. Since the HMT is particularly well suited to images containing singularities, it provides a good classifier for distinguishing between textures. Utilizing the inherent tree structure of the wavelet HMT and its fast training and likelihood computation algorithm, texture classification at a range of different scales is attempted. These multi-scale classifications are fused using a Baysian probabilistic graph to obtain reliable final segmentation. The performance of the algorithm has been experimentally proved for a number of images like synthetic, aerial photo and document image segmentations. Unser and Murray Eden (1989) discussed the multi resolution feature extraction and selection for texture segmentation

2.5 APPLICATIONS

Texture refers to the innate surface properties of an object and their relationship to the surrounding environment. A texture pattern evolves due to the surface finish characteristics or the variation in the reflectance property of the real objects. The images of the real objects exhibit such texture patterns as intensity variation of pixels over a spatial support. An analysis of texture finds a variety of applications in the areas of remote sensing, medical image analysis, automated inspection, document processing, and image retrieval. Any real-world image consists of regions of homogeneous texture. The heterogeneity among these regions is used for classification of categories such as forest, habitation, agricultural land in satellite images and white matter, gray matter and CSF (cerebro-spinal fluid) in a brain image. The texture features undergo a fluctuation across the boundary separating two homogenous texture regions. This fact can be used to perform segmentation of medical images. Texture information is also used for browsing and retrieval of large image data. There are so many application areas for texture analysis, such as remote sensing, industrial applications, medical image analysis etc. (Heaton et al 1990; Varma et al 2002 and Vibha et al 2006). Since we have undertaken skin image analysis for an application of our proposed texture representation, the following sub sections give a brief review of medical and skin image analysis followed by various other applications also.

2.5.1 Medical Image Analysis

Medical applications often involve the automatic extraction of features of the image for performing classification tasks, such as distinguishing normal tissue from abnormal tissue. Textural properties are

widely used to develop such automated medial diagnostic system to aid the radiologists.

Lung diseases such as interstitial fibrosis exhibit some textural changes in the x-ray images. Sutton and Hall (1972) used texture features such as isotropic contrast measure, directional contrast measure and Fourier domain energy sampling to distinguish normal lungs from diseased lungs. In their experiments, the directional contrast measure produced the best classification results.

Ginneken et al (2002) presented a fully automatic scheme for texture analysis of lung fields in chest radiographs. The images are segmented and features are extracted from histograms of the responses of multi-scale filter banks. The image database consists of 616 chest radiographs and the classification results are fairly accurate, in identifying cases of active tuberculosis (TB).

Chen et al (1989) employed fractal texture features to classify ultrasound images of livers and used the same to do edge enhancement in chest x-rays. Mir et al (1995) investigated whether texture could be used to discriminate the various tissue types that are inaccessible to human perception. They succeeded in early detection of malignancy in the liver CT images, using the features namely entropy, local homogeneity and gray level distribution, with a confidence level of above 99%. Jeong and Kim (1996) reported that classification with multi texture feature vector was better with 10% higher classification rate than single texture feature methods. They used 27 texture feature vectors, out of which 12 vectors had been selected as the best ones with the help of the Bhattacharya distance and the Hoteling trace criterion (HTC). Multi-texture feature vector classifiers were then used to classify the images into normal and cirrhosis liver.

Glestos et al (2001) developed a neural network-based diagnostic system using 48 texture features in order to classify four hepatic tissue types namely normal liver, hepatic cyst, hemangioma and hepatocellular carcinoma. The classifier used in their work consists of three sequentially placed feed forward neural network. The first neural network classifies the liver regions into normal and pathological ones. The pathological liver regions are classified by the second neural network into cysts or "other disease". The third neural network classifies "other disease" into hemangiomas and hepatocellular carcinomas. A total correct classification rate of 98% was reported.

Prostate cancer (especially in men) is the second leading cause of death worldwide. Mohamed et al (2003), attempted to diagnose prostate cancer by using texture features derived from tansrectal ultrasound (TRUS) images. Texture features from the images are extracted by multi channel Gabor filters and a K-means clustering algorithm segments the TRUS images into regions.

Plaques in the carotid artery increase the possibility of a stroke in patients. A Carotid endarterectamy operation will reduce the incidence of a stroke. Since all the plaques are not symptomatic, it is necessary to develop methods to identify the asymptomatic plaques. Christodoulou and Pattichis, (2003) employed texture-based classification to characterize the carotid plaques for identification of individuals with asymptomatic carotid stenosis, who run the risk of a stroke. The data they utilized, consists of 115 symptomatic and 115 asymptomatic carotid plaque ultrasound images. Nine different sets of texture features have been used as inputs to two types of classifiers namely neural network self- organizing map (SOM) and statistical 'K' nearest neighbor (KNN). The entire feature sets performed in a range of about 62%-70% correct classification. Combining the results of the SOM

classification of all the feature sets, increased the correct classification to 73%.

Texture analysis techniques for the classification of micro calcifications in digitized mammograms are dealt with, by Dani Kramer and Furzin Aghdasi 1999; Al-Hinnawi et al 1997. Clustered micro calcifications on X – Ray mammograms are an important clue for early detection of breast cancer. A neural network based texture analysis method has been used by in Catherine M. Kocur et al 1996; Jong Kook Kim and Hyun Wook Park 1999; Mala and Sadasivam 2005. The fuzzy neural network classifier for the characterization of ultrasonic liver images based on texture analysis techniques is investigated by Pavlopoulos et al 1996. Classification features are extracted with the use of image texture analysis techniques such as fractal dimension texture analysis and spatial gray level dependence matrices etc.

Computer assisted characterization of liver tissue using image texture analysis techniques on B scan images (Kyriacou et al 1998) and quantitative characterization of ultrasonic liver images (Kyriacou et al 1997) have been presented. An analysis of ultra sound speckle texture provides information about the underlying properties of tissue, which could find applications in early lesion detection and tissue characterization (Di Lai et al 2007).

2.5.2 Skin Image Analysis

The skin is a complex landscape that is difficult to model for many reasons. Reflection and inter reflection of light affect the complex optical properties of skin layers as well as the surface micro geometry of pores and wrinkles. As with many real world surfaces, skin appearance is strongly affected by the direction from which it is viewed and illuminated.

Skin surface is texture, i.e. a texture in which the fine scale geometry affects the overall appearance. Increasingly, recent works (Chantler 1995; Koenderink and van Doorn 1996; Van Ginneken et al 1999; Suen and Healey 2000; Mc Gunnigle and Chantler 2000; Leungand Malik 2001; Zalesny and van Gool 2001; Penirschke et al 2002; Pont and Koenderink 2002; Cula and Dana 2002; Cula and Dana 2003) address this type of texture and its variation with viewing and illumination direction. The terminology for texture that depends on imaging parameters was introduced by Dana et al 1997; Dana et al 1999. Specifically, the term bidirectional texture function (BTF) is used to describe image texture as a function of the four imaging angles (viewing and light source directions). The BTF is analogous to the bidirectional reflectance distribution function (BRDF). While BRDF is a term for the reflectance of a point, most real world surfaces exhibit a spatially varying BRDF and the term BTF is used for this situation.

Simple models of skin appearance are not sufficient to support the demands for high performance algorithms in computer vision and computer graphics. For example, in computer vision, algorithms for face recognition, shape estimation and facial feature-tracking rely on accurately predicting appearance so that local matching can be done among images obtained with different imaging parameters. In computer graphics, the popular technique of image-based rendering (typically) creates new views of local texture by warping reference images. This approach cannot capture local variations in occlusions, foreshortening and shadowing due to the fine scale geometry of textured surfaces. Therefore skin renderings lack realistic surface detail. Other methods are designed specifically for rendering skin texture: (Ishii et al 1993; Nahas et al 1990; Boissieux et al 2000) but a truly accurate synthesis of skin and the changes that occur with imaging parameters is still an open issue. Although much work has been done in modeling for facial animation (Lee et al 1995; Guenter et al 1998; DeCarlo et al 1998; Blanz and Vetter 1999),

accurately rendering surface detail has not been the primary emphasis and remains an open topic.

In addition to computer vision and graphics, accurate skin models may be useful in dermatology and several industrial fields. In dermatology, these skin models can be used to develop methods for computer-assisted diagnosis of skin disorders. In the pharmaceutical industry, quantification is useful when applied to measure the healing progress. Such measurements can be used to evaluate and compare treatments and can serve as an early indicator of the success or failure of a particular treatment course. Consumer products and cosmetic industries can use computational skin representations to substantiate claims of appearance changes.

Skin appearance was measured and an image-based texture representation (Oana G. Cula and Dana 2002) applied for skin classification. The techniques used, enable classification of textured surfaces of unknown viewing and illumination directions. The observed skin appearance changes significantly with changes in viewing and illumination direction, because the surface micro geometry introduces local occlusion, shadowing, and foreshortening. Features apparent in one view seemingly disappear in another image, while new features reappear. This multi view approach (that is many images characterize the surface) provides a more comprehensive surface representation than any single image texture representation.

2.5.3 Remote Sensing

A growing amount of remote sensing data is available today from different types of sensors. A certain level of automation can speed up the information processing considerably. The vital applications of remote sensing technology included identification and classification of vegetation, soil types,

water courses, roadways, water content of underlying terrain, clouds, mineralogical and chemical composition of dry surface rocks, subsurface fresh water runoff into the ocean, ice depth, snow cover, map updating etc. Texture analysis has been extensively used to classify remotely sensed images.

Augesteijn et al (1995) compared various texture measures such as co-occurrence matrices, gray-level differences, texture tone features and features derived from Fourier spectrum and Gabor filters. A thematic Mapper (TM) image in six bands, showing nine different ground cover classes was used in this study. It has been concluded that the performance of the Fourier measures ranks the highest. The co-occurrence features perform consistently for various feature dimensions. The computation time for co-occurrence features is relatively large. In another study by Schistad and Jain (1992), fractal dimension, autoregressive Markov Random Field (MRF) model and gray level co-occurrence texture features were used to identify land use categories in Synthetic Aperture Radar (SAR) images. It was reported that, the classification error was as low as 6% for the MRF features.

The classification of new forming ice and older ice from the SAR images has been performed by Deng et al (2003). Since new forming ice images have randomly rotated positions due to water current and pressure from the nearby masses, rotation-invariant texture features are required for the task of classification. The authors developed an Anisotropic Circular Gaussian MRF (ACGMRF) model for rotated image textures, which yielded a 95.22% classification rate for new forming ice while the rotation variant GMRF yielded 58.81% only. Christodoulou et al (2003) utilized texture analysis methods for the classification of clouds into six types, namely, altocumulus-altostratus (ACAS), Cumulonimbus(CB), Cirrus-cirrostratus (CICS), Cumulus-stratocumulus (CUSC), Stratus (ST) and Clear Conditions

(CLEAR) based on their shape and distance from the land. Nine feature sets have been employed. The spatial gray level dependence matrices (SGLDM) outperformed others with a correct classification rate of 60.7%. The classification rate improved to 64.2%, when the classification results of the nine different feature sets are combined.

Dekker (2003) employed texture measures such as histogram measures, wavelet energy measures, fractal dimension, lacunarity and semi variogram for map updating of urban areas in The Netherlands. The SAR image obtained from European Remote Sensing satellite 1, was used to update the digital map to 1:250,000 maps (100 image pixels per map centimeter).

2.5.4 Inspection

Texture has been used in automated inspection problems such as defect detection in images of textiles, carpet wear assessment, paint quality assessment etc. Textile defects are categorized as point defect, band defect and line defects. Dewaele et al (1998) proposed self-adaptive convolution filters specific to the type of fabric texture. Texture features are extracted from the filtered image. A Mahalanobis distance classifier is used to classify the defective areas. Cristobal et al (2003) adopted the spectral method for detection of fabric defective textures and epithelial cell cultures. Pseudo Wagner Distribution (PWD) gives a simultaneous representation of a signal in space and spatial frequency variables. In this work, the high-resolution joint representation of PWD is exploited. Since PWD suffers from high redundant information, a neural based principal component analyzer (PCA) is used as a fast and adaptive spectral decorrelator. The classification of defective areas is performed with the reduced data.

Siew et al (1988) have effectively utilized texture analysis procedures such as spatial gray level dependence matrix (SGLDM), Gray level difference method (GLDM), and Gray level Run Length Matrices (GLRLM) to numerically characterize the appearance of carpets. The changes in the carpet texture are attributed to the wear the carpet undergoes. It has been shown that NGTDM has a strong classification power. An automatic system for the inspection and classification of marble slabs in production line according to their texture is presented by Juan et al 1999. The sum and difference histogram features are extracted from the images of the marble slabs and statistical information is computed over the Histogram features to reduce the dimensionality. A Linear Vector Quantising (LVQ) is trained to classify the marble slabs of type "Crema Marfil Sierra de la Puerta" into subclasses according to their texture.

2.5.5 Document Processing

The first step in document processing applications is to separate the useful information contained in the image from the background. More specifically, the task is a segmentation problem to achieve text-graphics separation, address block location, bar code localization etc. Most of the works in the area of document processing are based on morphological characteristics, connect component analysis, Hough transform techniques etc. Jain et al (1992) applied the texture segmentation method to achieve the same. They employed eight Gabor filters corresponding to the two radial frequencies (μ_0 = 64/√2 and 32/√2 cycles/image) and four orientations (θ = 0°,45°,90°,135°). The homogeneous regions in the feature image are found in an un-supervised mode (clustering) or a supervised mode (classification). In an un-supervised mode, three clusters are grouped. One cluster corresponds to patterns belonging to the text, the second represents uniform regions such as blank spaces and pictures of slow intensity variations,

and the third cluster represents the boundaries or transition areas between the two types of regions. This work demonstrates the effectiveness of the texture segmentation method for document processing.

2.5.6 Image Retrieval

Image data base systems traditionally access images using keywords or the text associated with the images. Unfortunately, it is often difficult to assign textual descriptions to images and consequently text-based queries often fail. The recent emergence of multimedia databases and digital libraries prompts researchers to find more optimal solutions for this problem. The task of manually annotating the large volume of imagery would involve a lot of time and expense. This leads to the development of image retrieval by allowing queries based on image content. Users can specify a search using image properties such as shape, color or texture.

Manjunath and Ma (1996) demonstrated a Gabor wavelet based texture analysis scheme to retrieve from a texture database of 1856 images. The Gabor features give the best performance, close to 74% retrieval. In comparison to that, the pyramid structured wavelet transform yields 68.7% retrieval, and the tree structured wavelets achieve 69.4%, while the multi-resolution autoregressive model reaches 73%.

$$BDIP = \frac{M^2 \sum_{i,j \in B} I(i,j)}{\max_{i,j \in B} I(i,j)} \tag{4.45}$$

Kim et al (2000) proposed invariant texture features for retrieval applications. Normalized DFT (Discrete Fourier Transform) computed from the texture image is invariant to scale and translation. The rotational

invariance is accomplished by extracting the Zernike moments from the DFT coefficients. Zernike moments are inherently rotation invariant. The Total Average Retrieval Rate (TARR) of the proposed features is shown to be more, compared to the Gabor, Radon and wavelet features. Chun et al (2003) reported two texture features, namely, Block difference of inverse probabilities (BDIP) and block variation of local correlation coefficient (BVLC) to yield about 12% better performance than the wavelet moments. BDIP is defined as the difference between the number of pixels in a block and the ratio of the sum of pixel intensities in the block to the maximum in the block.

BVLC is expressed as,

$$BVLC = \max_{(k,l)}[\rho(k,l)] - \min_{(k,l)}[\rho(k,l)] \tag{4.46}$$

where,

$$\rho(k,l) = \frac{\frac{1}{M^2}\sum_{(i,j)\in B} I(i,j)\,I(i+k,j+l) - \mu_{0,0}\,\mu_{k,l}}{\sigma_{0,0}\sigma_{k,l}} \tag{4.47}$$

where I(i, j) denotes the pixel intensity at (i, j) and ‘B’ is a block of size M×M.

$\mu_{0,0}$ and $\sigma_{0,0}$ denote the local mean and standard deviation of the block of size M×M respectively. The notation (k, l) denotes the four orientations (-90°, 0°, -45°, 45°). The first and second moments of BDIP and BVLC form the feature vector. The system finally calculates the distance between the feature vector of the query image and that of each target image in

an image database and retrieves a given number of the most similar target images.

2.6 SUMMARY

In this chapter, a detailed survey of the reported literature on various texture analysis methods such as statistical, structural, model-based and transform methods has been presented. The various applications of texture methods have also been discussed. The motivation behind this research work is that there are not many works reported on combining the statistical and structural principles for texture representation. Since texture perception is closely related to the understanding of the human visual system, ample scope exists for developing new methods of texture analysis by combining both the paradigms for texture representation. Moreover, no single method can be appropriate for all types of texture images. Hence, the aim of this research is to develop texture analysis schemes based on combined statistical and structural approaches. The mathematical model for the proposed work for texture description in local and global experimentation will be discussed in the next chapter.